Available online at www.sciencedirect.com
ScienceDirect
Carbohydrate Research 343 (2008) 350–363
Carbohydrate RESEARCH

The effect of sodium chloride on molecular mobility in amorphous sucrose detected by phosphorescence from the triplet probe erythrosin B

Yumin You and Richard D. Ludescher*

Department of Food Science, Rutgers, The State University of New Jersey, 65 Dudley Road, New Brunswick, NJ 08901-8520, USA

Received 25 June 2007; received in revised form 2 November 2007; accepted 6 November 2007
Available online 13 November 2007

Abstract—Phosphorescence from the triplet probe erythrosin B provides spectroscopic characteristics such as emission energy and lifetime that are specifically sensitive to molecular mobility of the local environment. This study used phosphorescence of erythrosin B to investigate how variation in NaCl content modulated the mobility of the amorphous sucrose matrix over the temperature range from 5 to 100 °C. Addition of NaCl increased the emission energy and the energy difference with excitation at the absorption maximum and the red edge, and increased the lifetime by reducing the non-radiative decay rate in the glass as well as in the undercooled liquid in a concentration dependent manner, indicating that NaCl decreased the matrix molecular mobility. Emission energy and lifetime increased with increasing NaCl content up to a maximum at NaCl/sucrose mole ratio of ~0.5; above 0.5 mole ratio, the effect of NaCl was less significant and appeared to be opposed by increasing plasticization by residual water. Changes in the width of the distribution of the emission energy and lifetime and variation in the lifetime with excitation and emission wavelength indicated that NaCl increased the spectral heterogeneity and thus increased the extent of dynamic site heterogeneity. These results are consistent with a physical model in which sodium and chloride ions interact with sucrose OH by ion–dipole interactions, forming clusters of less mobile molecules within the matrix.

Keywords: Sucrose; NaCl; Amorphous solid; Molecular mobility; Phosphorescence; Erythrosin B

1. Introduction

Vitreous sugar systems are important in the preservation of seeds, spores and even living organisms under extreme conditions because sensitive biomaterials such as proteins or nucleic acids have increased stability when embedded in an amorphous, non-crystalline solid.[1–3] Sugars readily vitrify upon rapid drying of solutions or cooling the concentrated liquid due to the enormous increases in viscosity that occur upon increasing the aqueous sugar concentration or lowering temperature. During vitrification, liquid sugar changes from a viscous solution into a hard, brittle and rigid glass characterized by a glass transition at temperature T_g. Glass formation involves a dynamic transition in the rates of translational as well as rotational and vibrational molecular mobility;[4] the glass transition reflects the onset temperature for translational molecular motion that supports viscous flow.

The glassy state of sugars and carbohydrates also plays an important role in modulating the stability and shelf life of dry and frozen foods and pharmaceuticals.[5–7] The ability of sugars to protect biomaterials from freeze-thaw damage and to provide long-term storage stability has attracted researchers to investigate the mechanisms of vitrification and to develop solid state

Abbreviations: Ery B, erythrosin B; FWHM, full width at half maximum; T_g, glass transition temperature; T'_g, glass transition temperature of the maximally freeze-concentrated solution

* Corresponding author. Tel.: +1 732 932 9611x231; fax: +1 732 932 6776; e-mail: ludescher@aesop.rutgers.edu

0008-6215/$ - see front matter © 2007 Elsevier Ltd. All rights reserved.
doi:10.1016/j.carres.2007.11.005

formulations, through drying or freeze-drying, for the labile compounds of foods, such as vitamins and flavor compounds, and pharmaceuticals, such as enzymes, antibodies, and other proteins.

Salts, which are universally present in biological systems and food products, have a major influence on water structure and possible interactions among hydrogen bonding and charged biomolecules. The effect of salts on the thermodynamic properties of aqueous solutions and the structure of water has been a topic of intense research since the pioneering studies of Hofmeister.[8] However, the effect of salts on sugar glasses has received little attention. Most of the research to date has investigated the mechanism by which salts, especially inorganic salts, inhibit crystallization in supercooled or freeze-dried sugar systems. Izutsu and Aoyagi, who studied the effect of different inorganic salts on crystallization of poly(ethylene glycol) in frozen solutions, found that salts inhibit the crystallization by altering molecular interactions and reducing molecular mobility; the level of inhibition depends on the type of salt and concentration.[9] NaCl increases the solution viscosity, promotes the formation of amorphous, glassy systems, and prevents crystallization;[10] the delayed crystallization may result from the effect on the nucleation mechanism of ion-induced microheterogeneities in the supercooled solutions.

A few studies have explored how salts modifies the glass transition temperature of freeze-dried systems. Shalaev et al. studied the properties of pharmaceutically compatible buffers at sub-zero temperatures in lyophilized formulations and found that the T'_g of a freeze-dried system (the glass transition temperature of the maximally freeze-concentrated solution) results from a competition between two opposite actions: increased viscosity due to an increase in the electrostatic interaction and decreased viscosity due to an increase in the amount of unfrozen water.[11] In a study of the effect of salts on water sorption behavior and ice crystallization in aqueous sugar systems, Mazzobre et al. reported that salts can modify the properties of concentrated sugar solutions without altering T'_g and these effects are related to the charge/size ratio of the cations present.[12] Kets et al. used a modified DSC method to determine the T_g of freeze-dried sucrose–citrate mixtures.[13] They found that when residual water was removed from the mixture, the T_g of sucrose increased with citrate concentration despite the literature suggesting the opposite effect.[14,15] The T'_g is not directly applicable indicator to evaluate the matrix properties influenced by salt in this study, however, because the samples used for measurements were dried films with residual moisture less than 2% (data shown in Section 2). The influence of salts on the glass transition temperature of dry systems may be satisfactorily described using composition-dependent equations derived from free volume theory such as the Gordon–Taylor equation. However, the variance of T'_g in the salt-containing freeze-concentrated solutions may provide insight into the mechanism of the salt effect on the matrix.

The measurement of molecular mobility in amorphous sugars is of fundamental interest because it provides insight into the molecular mechanisms that control long-term stability. A number of techniques have been used to characterize the properties and mobility of amorphous materials including Fourier transform infrared (FTIR) spectroscopy,[16,17] dielectric relaxation,[18–20] differential scanning calorimetry,[13,21–24] nuclear magnetic resonance spectroscopy,[25] electron spin resonance,[26,27] and phosphorescence spectroscopy.[28]

Due to its high phosphorescence quantum yield, long lifetime, site selectivity, and high sensitivity, erythrosin B (Ery B) phosphorescence has been widely used to monitor the molecular mobility as well as dynamic site heterogeneity in amorphous solid sugars[29–32] and proteins.[33–37] In the present study, phosphorescence of Ery B was used to measure the matrix mobility in films of amorphous sucrose–NaCl mixtures. NaCl content was varied from 0 to 0.87 mole ratio of NaCl/sucrose by addition of NaCl to the concentrated sucrose solution prior to film formation. The temperature-dependence of mobility was measured and analyzed at different NaCl contents, generating families of mobility versus temperature curves. Comparisons thus provided insight into the mechanisms by which NaCl influences mobility in amorphous sucrose.

2. Results

At a probe/sucrose mole ratio of $1{:}10^4$, on average each probe is surrounded by a matrix shell approximately 10–11 sucrose molecules thick. Under these conditions, Ery B does not aggregate within the sucrose matrix and thus effectively reports the physical properties of the sucrose matrix.[38]

2.1. Delayed emission spectra

The delayed emission spectra of Ery B in amorphous sucrose and sucrose–NaCl films (data not shown) had a long wavelength phosphorescence band (maximum ~680 nm) reflecting emission from the triplet T_1 state and a short wavelength delayed fluorescence band (maximum ~555 nm) reflecting emission from the singlet S_1 state that has been repopulated by reverse intersystem crossing from the triplet state.[39] Delayed emission spectra collected over the temperature range from 5 to 100 °C showed the expected decrease in phosphorescence and increase in delayed fluorescence intensity with increasing temperature; in addition, both the delayed fluorescence and phosphorescence band shifted

to longer wavelength at high temperature. The intensity ratio $\ln(I_{df}/I_p)$ was plotted versus $1/T$ and the slope used to estimate the energy gap ΔE_{TS} between T_1 and S_1 (Eq 6, Section 5). In pure sucrose ΔE_{TS} was 31.56 ± 0.56 kJ mol^{-1} whereas in sucrose–NaCl films with mole ratios from 0.04 to 0.87, ΔE_{TS} was 30.77 ± 0.67, 31.12 ± 0.58, 31.21 ± 0.18, 30.80 ± 0.52, 30.65 ± 0.48, 30.15 ± 0.32, 30.85 ± 0.50, 30.44 ± 0.26, and 29.93 ± 0.37 kJ mol^{-1}, respectively, indicating that NaCl induced a slight, but perhaps not significant, decrease in the singlet–triplet energy gap.

The peak frequency (ν_p) and bandwidth (Γ) for both delayed fluorescence and phosphorescence emission were determined by fitting to a log-normal line shape function (Eqs 1 and 2); the values of ν_p and Γ for phosphorescence are plotted in Figure 1a and b, respectively. The peak frequency and bandwidth for delayed fluorescence displayed similar behavior (data not shown). The phosphorescence peak frequency in both pure sucrose and sucrose–NaCl mixtures decreased biphasically as a function of temperature; ν_p decreased gradually at low temperature and more steeply at high temperature. The extent of the decrease in peak frequency from 5 to 100 °C increased with NaCl content in a concentration-dependent manner. For pure sucrose, $\Delta\nu$ ($=\nu_{5\,^\circ C} - \nu_{100\,^\circ C}$) was $\sim$340 cm^{-1} while in sucrose–NaCl mixtures $\Delta\nu$ increased from 400 cm^{-1} at a mole ratio of 0.065 to 513 cm^{-1} at a mole ratio of 0.87. The decrease in emission energy ν_p with increasing temperature reflects an increase in the average extent of dipolar relaxation around the excited triplet state prior to emission.[40,29] The increase in the energy difference $\Delta\nu$ with NaCl content suggested that the effect of temperature on the rate of dipolar relaxation increased with NaCl content.

The phosphorescence bandwidth increased biphasically as a function of temperature in both pure sucrose and sucrose–NaCl mixtures; Γ increased gradually at low temperature and more steeply at high temperature. The increase in bandwidth reflects an increase in the extent of inhomogeneous broadening of the Ery B emission spectra, indicating that at higher temperature there is a corresponding increase in the range of energetically distinct matrix environments in the amorphous sucrose–NaCl mixtures.

The spectra of Ery B were blue-shifted (ν_p increased) in the presence of NaCl in a complex, concentration-dependent manner (Fig. 2a). The peak frequency increased steeply with NaCl content over the range from 0 to 0.09 mole ratio of NaCl/sucrose, increased gradually with NaCl content over the range from 0.09 to 0.46, and decreased gradually at higher mole ratios. The total increase in emission energy over the range from 0 to 0.46 mole ratio was greater at low than at high temperature while the decrease in emission energy from 0.46 to 0.87 was greater at high than at low temperature. The maximum peak frequencies over the whole temperature range were observed at a NaCl/sucrose mole ratio of 0.46. The emission bandwidth also varied with NaCl content in a concentration-dependent manner (Fig. 2b), increasing with NaCl content up to a mole ratio of 0.36–0.46, and then decreasing slightly at higher mole ratios. The effect of NaCl on bandwidth was greater at high than at low temperature.

2.2. Red-edge effect

Measurements of the red-edge effect as a function of temperature in both sucrose and sucrose–NaCl films are plotted in Figure 3 as the energy difference ($\Delta\nu_p$) of the Ery B emission band maximum with 530 nm and 560 nm excitation. The magnitude of $\Delta\nu_p$ provides a qualitative measure of the extent to which the matrix can relax around the excited state prior to emission; larger values of $\Delta\nu_p$ indicate the presence of matrix relaxation times that are slow compared to the excited state lifetime.[41] The magnitude of $\Delta\nu_p$ decreased gradually at low and more steeply at high temperature in pure sucrose and in films with NaCl/sucrose ratios of 0.04, 0.44, and 0.53, suggesting that the rate of matrix relaxation increased with temperature in both the pure sucrose and sucrose–NaCl films. The energy difference increased with increasing NaCl concentration over the range from 0 to 0.53 mole ratio at all temperatures from 5 to 85 °C. All the curves exhibited a break point, sucrose at 58 °C and NaCl–sucrose with mole ratios of 0.04, 0.44, and 0.53 at temperatures of 60, 61, and 63 °C, respectively. The slopes of the sucrose–NaCl curves became less negative than that of sucrose at higher temperatures; addition of NaCl thus reduced the rate of matrix relaxation within the sucrose glass and more significantly in the sucrose undercooled liquid.

2.3. Phosphorescence decay kinetics

Phosphorescence intensity decays of Ery B in sucrose–NaCl glasses were measured over the temperature range from 5 to 100 °C. As expected for Ery B in amorphous sucrose,[29,38,42] all decays were well-fit with a stretched exponential decay model (Eq 3). The stretched exponential lifetimes (τ) and stretching exponents (β) are plotted as a function of temperature in Figure 4. The lifetimes decreased biphasically with increasing temperature, exhibiting a gradual linear decrease at low and a more dramatic decrease at high temperature. The lifetimes varied with NaCl content, increasing over the range from 0 to 0.46 mole ratio and either remaining approximately constant (at low temperatures) or decreasing slightly (at higher temperatures) at higher mole ratios.

The stretching exponent β varied with temperature in all sucrose–NaCl films; β was generally slightly smaller than the value in pure sucrose below 60 °C and slightly

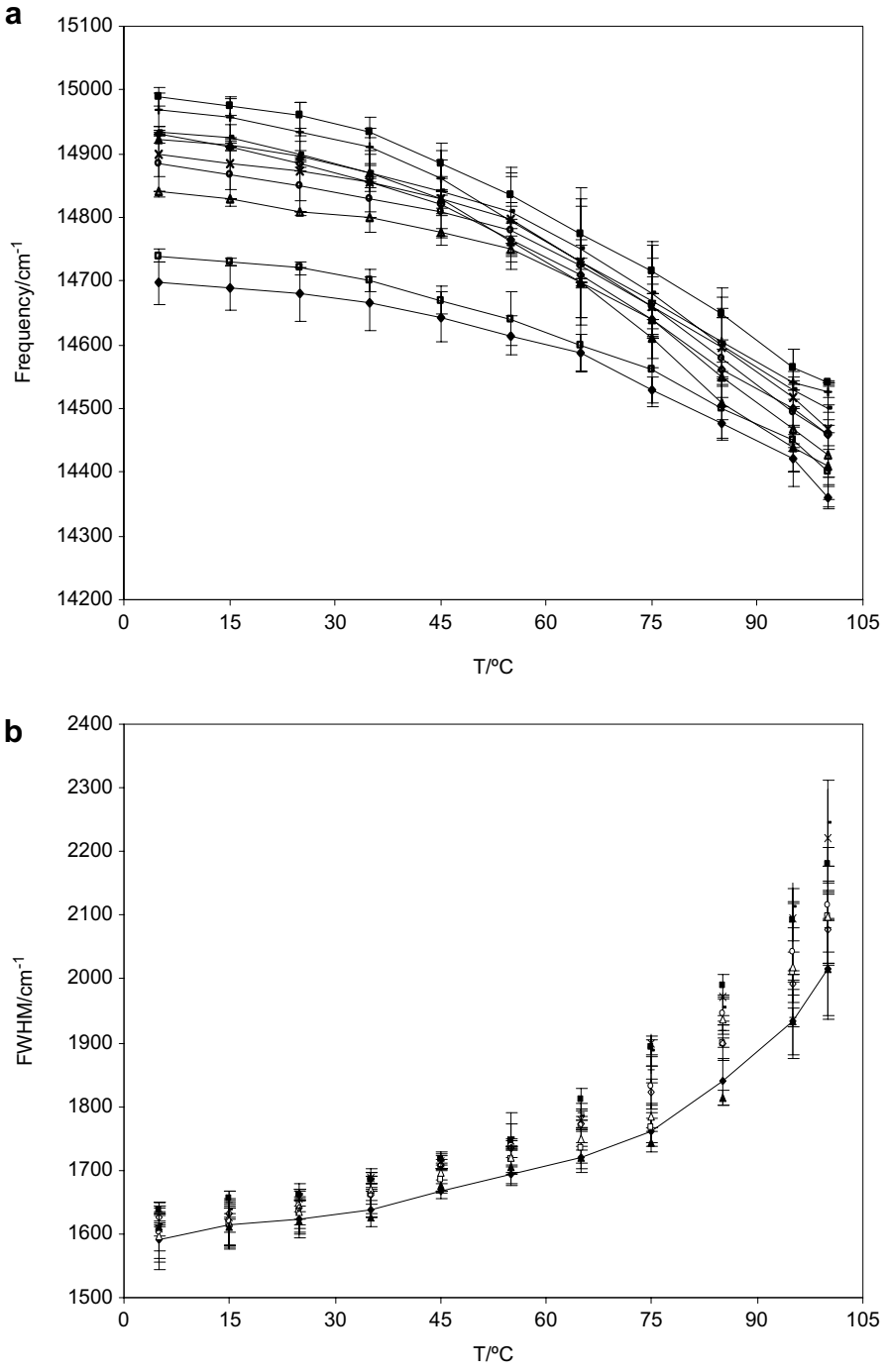

Figure 1. Effect of temperature on the peak frequency ν_p (a) and emission bandwidth Γ (b) of phosphorescence emission from erythrosin B in amorphous sucrose–NaCl films with various NaCl/sucrose mole ratios. Delayed emission spectra collected as a function of temperature were analyzed using a log-normal line shape function. NaCl/sucrose mole ratios were ◆, 0; □, 0.04; Δ, 0.065; ○, 0.09; ×, 0.20; –, 0.36; ■, 0.46; +, 0.56; ◇, 0.73; and ▲, 0.87.

larger above 60 °C. This value is close to the glass transition temperature of ~63 °C for pure sucrose estimated using the equation for the dependence of T_g on moisture content developed by Crowe and collegues[43]; the T_g reported in the literature for sucrose varies from 52 to 70 °C[44] and the value of 68 °C was selected as the T_g for anhydrous sucrose.[13,21,44] Since β reflects the distribution of lifetimes and thus the corresponding distribution of dynamically distinct probe environments with different values of k_{TS0},[29] the small decrease in β with addition of NaCl at low temperature indicated a small increase in the range of dynamically distinct probe

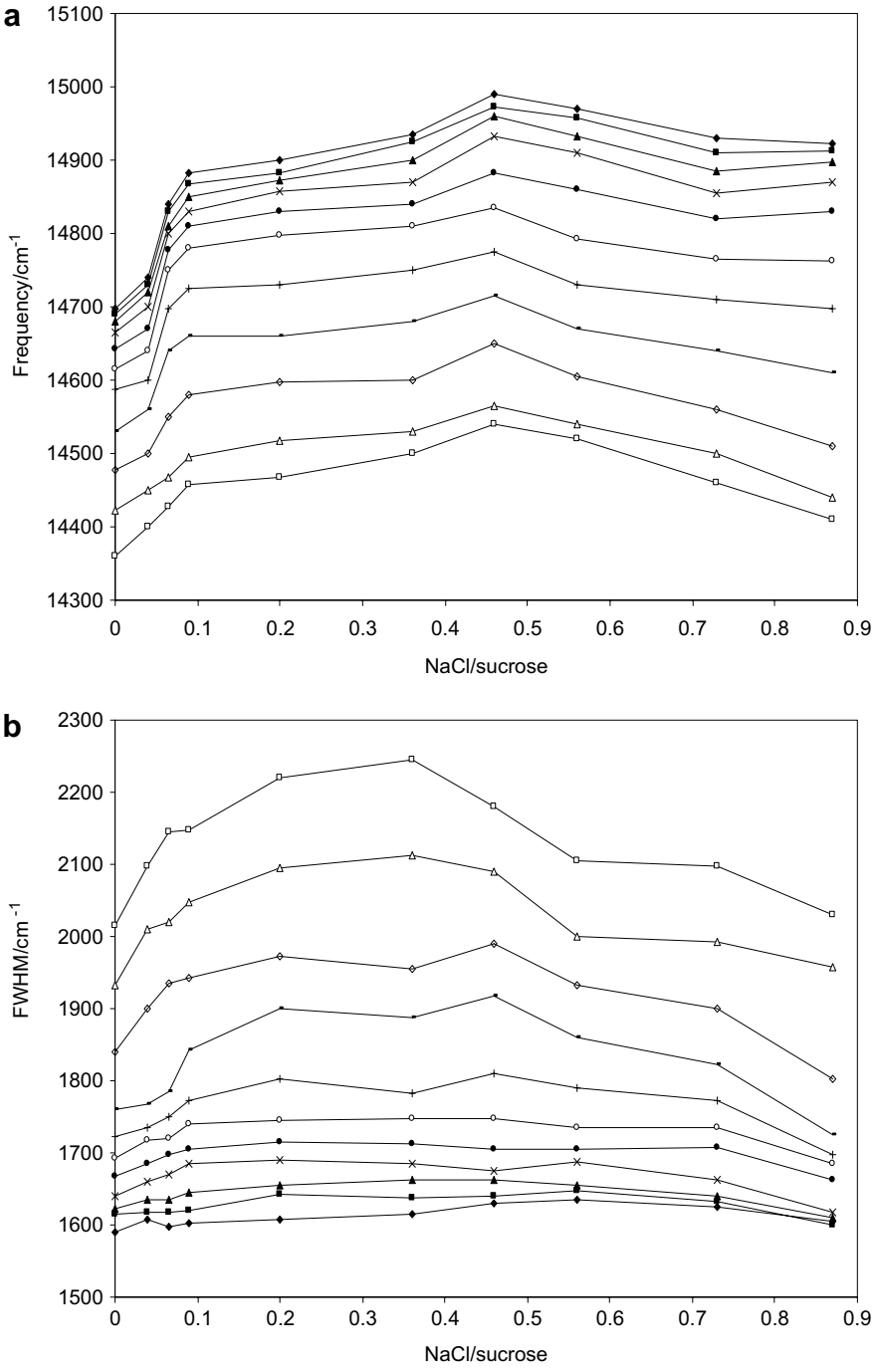

Figure 2. Peak frequency (a) and bandwidth (b) of phosphorescence emission from erythrosin B in amorphous sucrose–NaCl films replotted as a function of NaCl/sucrose mole ratio (data from Fig. 1). Temperature increased from top to bottom (a) and from bottom to top (b): ◆, 5 °C; ■, 15 °C; ▲, 25 °C; ×, 35 °C; ●, 45 °C; ○, 55 °C; +, 65 °C; –, 75 °C; ◇, 85 °C; Δ, 95 °C; and □, 100 °C.

environments in the glass and the larger increase in β at high temperature indicated a large decrease in the range of dynamically distinct probe environments in the undercooled liquid.

The decrease in lifetime with temperature reflects an increase in the rate of non-radiative decay of the excited triplet T_1 state due to an increase in both the rate of intersystem crossing to the ground state S_0 (k_{TS0}) and the rate of reverse intersystem crossing to S_1 (k_{TS1}).[29] Based on our estimate of the maximum physically reasonable value of k_{TS1},[29] the lower limit of k_{TS0} was calculated using Eq 7 (Section 5); these data are plotted as $\ln(k_{TS0})$ versus $1/T$ in Figure 5. The variation in k_{TS0} was small at low temperature and increased dramatically at high temperature, indicating that this rate is sensitive to the molecular mobility activated at high temperature.

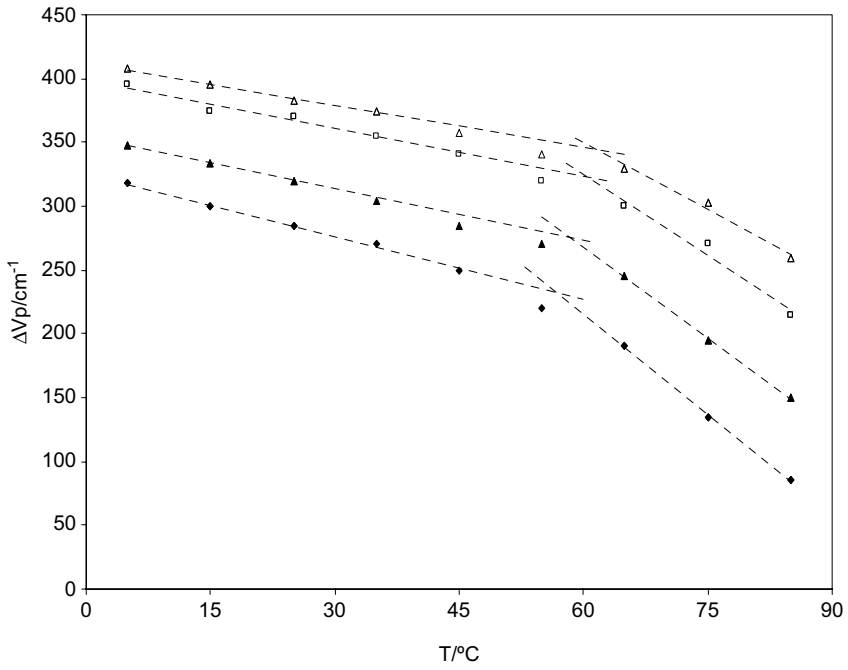

Figure 3. Effect of temperature on the red-edge effect for phosphorescence emission of erythrosin B in amorphous sucrose (◆) and in films with NaCl/sucrose mole ratios of 0.04 (▲), 0.44 (□), and 0.53 (Δ). $\Delta\nu_p$ is the difference in peak frequency of the emission band of the phosphorescence emission with excitation at 530 and 560 nm. The dotted lines used as a guide for eyes are plotted by extrapolating linear fits to the three data points at high and low temperatures, respectively.

Addition of NaCl decreased the quenching rate in both the glass and the undercooled liquid and, at mole ratios $\leqslant$0.56, enhanced the temperature at which the additional mobility was activated; at higher mole ratios (0.73 and 0.87) the quenching rate began to increase at a temperature lower than the sucrose T_g but k_{TS0} did not increase as much as in the other films.

The quenching rate k_{TS0} decreased continuously with added NaCl over the range from 0 to 0.46 mole ratio at all temperatures, decreasing more steeply at low mole ratio (0–0.09) and more gradually at higher mole ratio; the effect of NaCl at mole ratios >0.46 depended upon the temperature. The effect of NaCl on k_{TS0} over the range from 0 to 0.46 varied with the temperature and was more dramatic at high than at low temperature: addition of 0.46 mole ratio NaCl decreased k_{TS0} by ~15% at 45 °C and below and by ~42% at 95 °C and above.

2.4. Spectral heterogeneity

Phosphorescence intensity decays of Ery B in sucrose films with different NaCl content were measured as a function of excitation and emission wavelength at 25 °C. The stretched exponential lifetimes varied systematically with both excitation and emission wavelength (Fig. 6a). In sucrose, the lifetime decreased across the emission band from a high of 0.65 ms at 640 nm to a low of 0.52 ms at 720 nm; lifetimes also decreased monotonically with increasing emission wavelength in sucrose–NaCl films. The lifetimes as well as the variation in lifetime across the emission band increased in the presence of NaCl. Lifetimes also varied across the excitation band at all NaCl contents, increasing with increasing wavelength to a maximum at 520–540 nm and then decreasing at higher wavelengths in both sucrose and sucrose–NaCl films.

The stretching exponent β also varied as a function of both excitation and emission wavelength (Fig. 6b) in both sucrose and sucrose–NaCl films. The values of β were usually, but not always, slightly lower in the presence of NaCl. In sucrose and sucrose–NaCl films β was lower at the blue edge of the emission band, increased with increasing wavelength to a maximum at 680–690 nm and then decreased slightly at the red edge. The variation of β across the excitation band in sucrose–NaCl films was similar to that in the sucrose film, generally increasing with wavelength.

The non-radiative quenching rate k_{TS0} varied systematically across both the excitation and emission bands in both sucrose and sucrose–NaCl films (Fig. 7). The addition of NaCl caused a decrease in k_{TS0} uniformly across both the excitation and emission bands.

3. Discussion

These measurements of the temperature dependence of the emission energy and lifetime of the Ery B probe dispersed in amorphous sucrose at different NaCl contents provide insight into various aspects of the solid-state

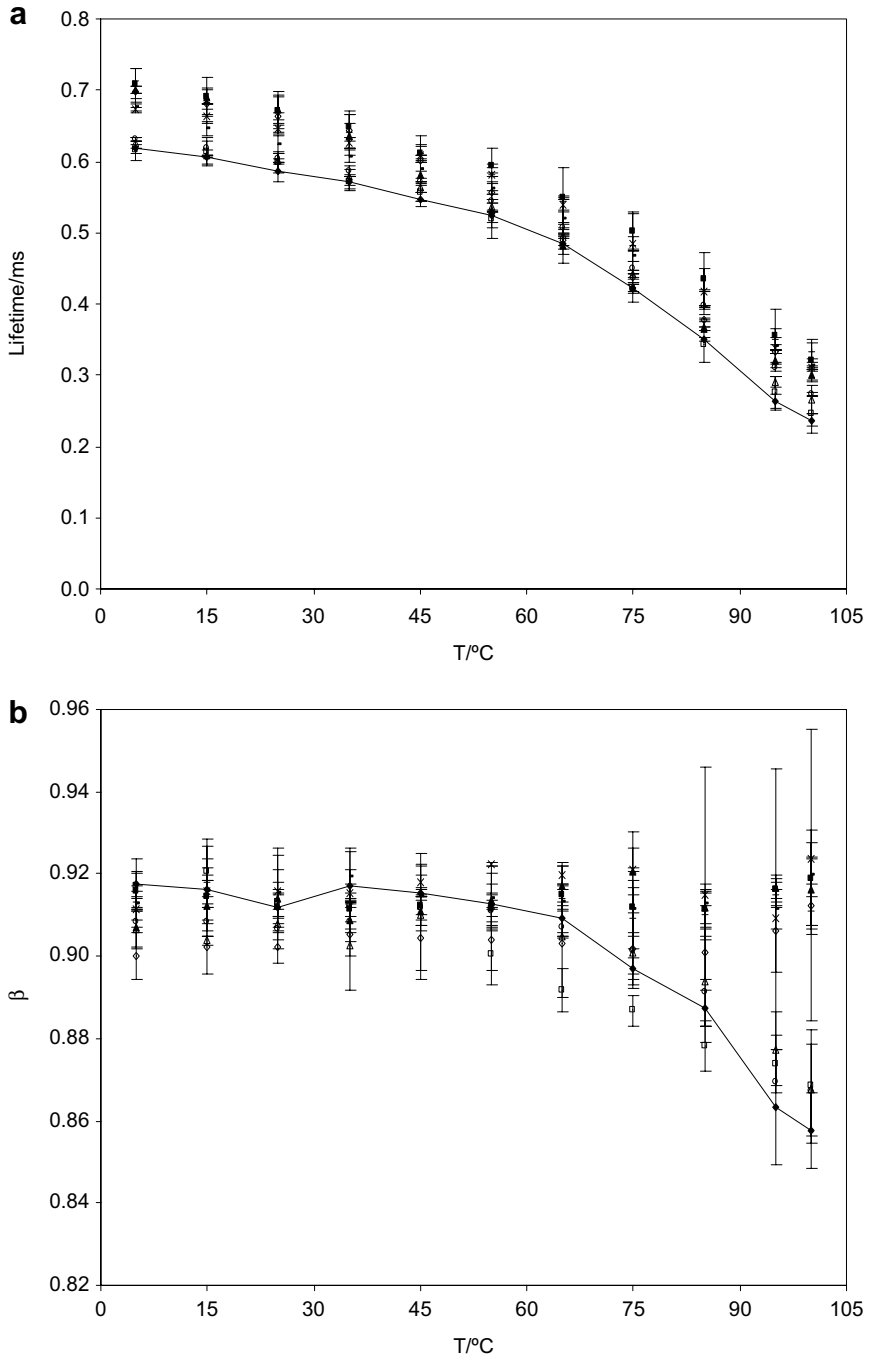

Figure 4. Effect of temperature on the phosphorescence lifetime τ (a) and stretching exponent β (b) of erythrosin B in amorphous sucrose with various NaCl/sucrose mole ratios (◆, 0; □, 0.04; Δ, 0.065; ○, 0.09; ×, 0.20; –, 0.36; ■, 0.46; +, 0.56; ◇, 0.73; and ▲, 0.87). Parameters were obtained from fits of intensity decays to a stretched exponential function.

biophysics of amorphous sucrose in the presence of an inorganic salt.

3.1. NaCl increased the molecular level rigidity of the sucrose matrix

NaCl increased the probe emission energy (peak frequency, v_p) and lifetime (τ) in a concentration-dependent manner in both the glass and the undercooled liquid. An increase in emission energy with a concomitant increase in probe lifetime indicates that NaCl decreased the rate of dipolar relaxation ($1/\varphi$), presumably of sucrose hydroxyl groups, around the excited triplet state;[31] a decrease in the rate of relaxation compared to the rate of emission leads to a decrease in the total extent of dipolar relaxation around the excited

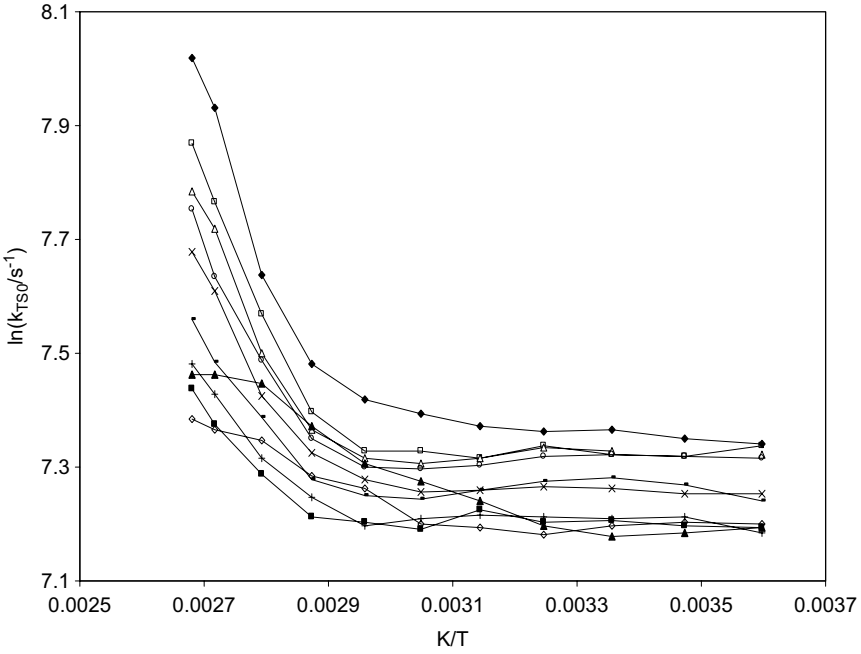

Figure 5. Arrhenius plot of the non-radiative decay rate (k_{TS0}) for the triplet state of Ery B in amorphous sucrose–NaCl films as a function of inverse temperature. NaCl/sucrose mole ratio varied from 0 to 0.87 (◆, 0; □, 0.04; Δ, 0.065; ○, 0.09; ×, 0.20; –, 0.36; ■, 0.46; +, 0.56; ◇, 0.73; and ▲, 0.87).

state and thus an increase in the average emission energy. The increase in lifetime reflects a decrease in the rate of collisional quenching (k_{TS0}) of the triplet state by the sucrose matrix;[29,32] the magnitude of k_{TS0} is sensitive to the extent of coupling of internal probe vibrational motions to external motions of the amorphous matrix and thus provides an indicator of overall matrix molecular mobility.[45,46] Addition of sodium chloride thus slowed the molecular mobility in the sucrose matrix in the glass at temperatures below T_g and in the undercooled liquid at temperatures above. The molecular rigidity of the matrix increased with increasing mole ratio of NaCl/sucrose over the range from 0 to 0.46 and kept approximately constant at higher mole ratios.

There are several possible physical consequences of adding NaCl to the sucrose films. As an electrolyte, sodium chloride strongly binds water. This is reflected by the higher residual water contents in samples with higher mole ratio NaCl; water content in the films increased from a low of 0.56 wt % in pure sucrose to a high of 2.34 wt % in films with 0.9 mole ratio NaCl/sucrose (see Section 5). Since an increase in water content will plasticize the matrix, and presumably increase the mobility, this cannot be the origin of the decreased mobility. It is also possible that NaCl crystallized within the amorphous solid matrix, forming microcrystals of NaCl (or perhaps NaCl·2H_2O)[47] that may, for some reason, lower matrix mobility. However, Shalaev et al., in their thermodynamic study of the ternary water–sucrose–NaCl system, found no evidence of NaCl crystals in frozen samples at weight ratios of sucrose/NaCl in excess of 6.[48] Since the weight ratio of sucrose/NaCl was always greater than 6.7 in our study (wt. ratio of NaCl/sucrose less than 0.149), it is unlikely that NaCl (or NaCl·2H_2O) crystals formed in the films. It thus appears that the presence of NaCl, as the associated molecule or as individual sodium and chloride ions, decreased the matrix mobility by modulating interactions among sucrose molecules. This direct dynamic effect of NaCl does not appear to reflect a change in the glass transition temperature.[48]

NaCl exhibited the greatest dynamic effect at a mole ratio of 0.46. The reason for this maximum is unclear. There are a number of studies of the effect of inorganic salts on the properties of sugar solutions; most report the existence of a 1:1 salt–sugar complex[47,49–52] while a few mention the existence of a 1:2 salt–sugar complex.[51,53] It may thus indicate that mobility is modulated by formation of a NaCl:sucrose complex. However, the maximum may reflect the serendipitous outcome of two contrary trends: a decrease in matrix mobility due to an intrinsic effect of salt and an increase in mobility due to an increase in water content in the high salt films. The water content was 0.56 ± 0.13, 1.04 ± 0.04, 0.81 ± 0.21, 1.06 ± 0.26, 1.04 ± 0.01, 1.18 ± 0.27, 0.54 ± 0.29, 2.17 ± 0.11, 2.32 ± 0.26, and 2.34 ± 0.25 wt % water in films with 0, 0.04, 0.065, 0.09, 0.20, 0.36, 0.46, 0.56, 0.73, and 0.87 mole ratio NaCl/sucrose, respectively, indicating that the water content was ~2-fold higher in films with greater than 0.46 mole ratio than in films with less. Given that the film with 0.46 mole ratio

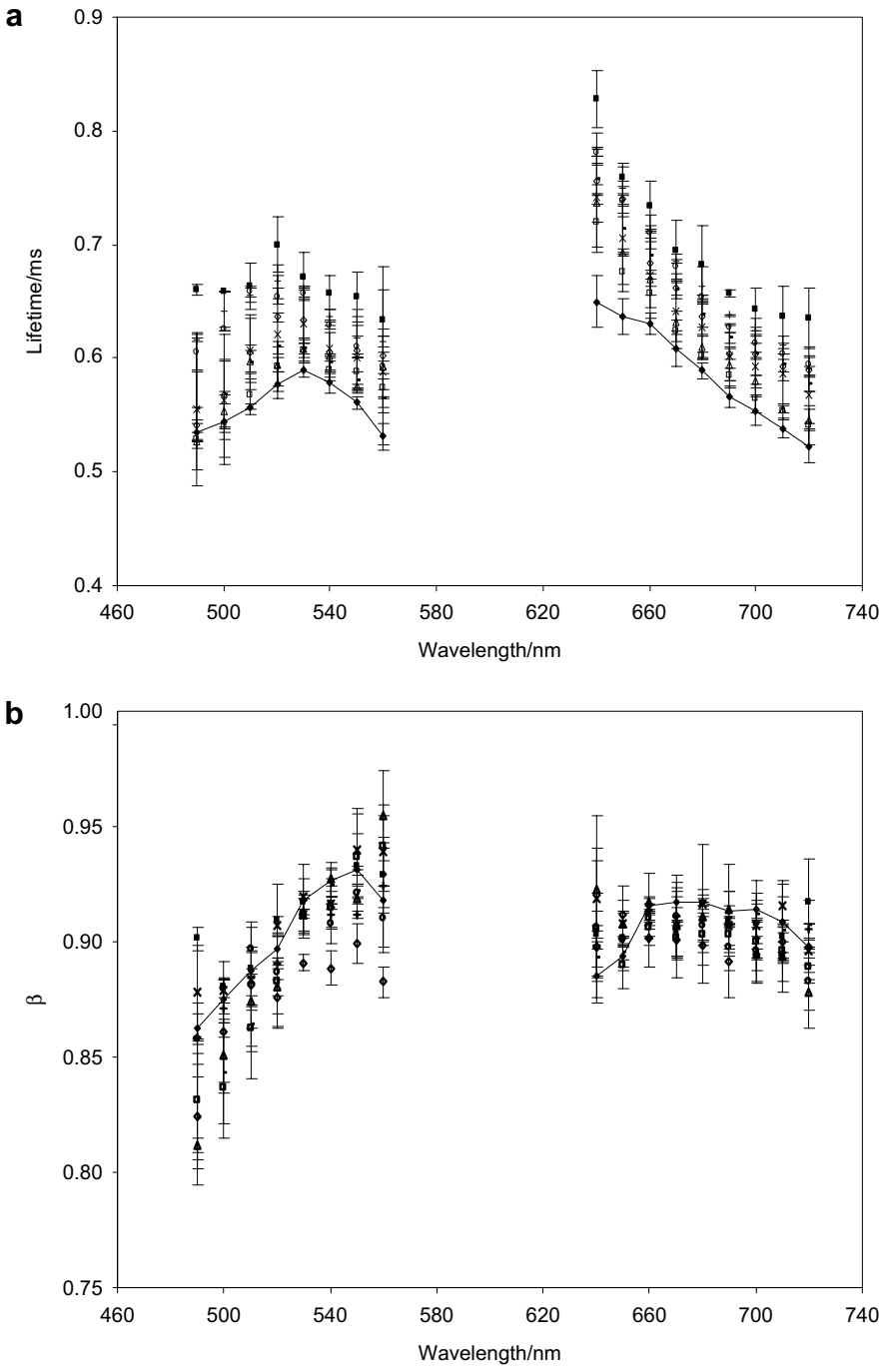

Figure 6. Effect of excitation and emission wavelength on the lifetimes (a) and stretching exponents β (b) from fits to the stretched exponential model of intensity decays of erythrosin B in amorphous sucrose film with various NaCl/sucrose mole ratios. Intensity decays were collected at 25 °C as a function of excitation wavelength (with 680 nm emission) and emission wavelength (with 530 nm excitation). NaCl/sucrose mole ratios were ◆, 0; □, 0.04; Δ, 0.065; ○, 0.09; ×, 0.20; –, 0.36; ■, 0.46; +, 0.56; ◇, 0.73; and ▲, 0.87.

NaCl/sucrose had the lowest water content (0.54 wt %), the low mobility in this film may merely reflect mobility in a drier matrix. Breaks in the lifetime data indicate that the films exhibited transition temperatures, calculated from the intersection of trendlines at high and low temperatures, of 76.5 °C in sucrose, and 75, 77, 77, 77, 79, 81, 79, 50, and 47 °C, respectively, in the films made with mole ratios from 0.04 to 0.87. The last two values are significantly below the glass transition temperature of the sucrose film, suggesting that water did plasticize the films with high NaCl content. However, since the 0.56 mole ratio sample with water content of

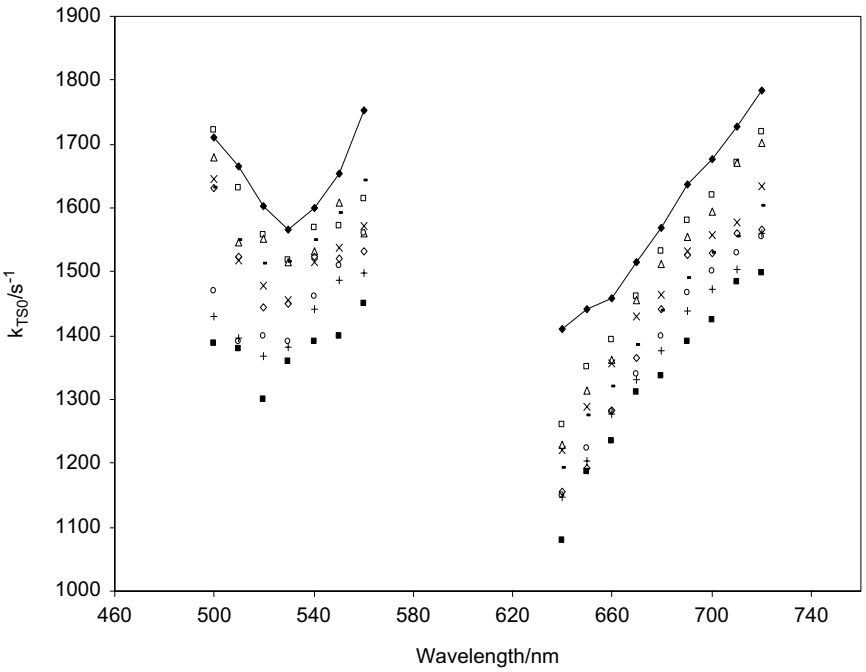

Figure 7. The rate constant for non-radiative decay of the triplet state to S_0 (k_{TS0}) plotted as a function of excitation wavelength (with 680 nm emission) and emission wavelength (with 530 nm excitation). Data collected at 25 °C from erythrosin B in sucrose films with NaCl/sucrose mole ratios of ◆, 0; □, 0.04; Δ, 0.065; ○, 0.09; ×, 0.20; –, 0.36; ■, 0.46; +, 0.56; ◇, 0.73; and ▲, 0.87.

2.17 wt % had an essentially unperturbed transition temperature of 79.2 °C, the evidence for plasticization by water is ambiguous.

The physical state of sucrose containing a very small amount of moisture becomes complicated due to the addition of a third component, NaCl. The miscibility/compatibility of the compounds in the ternary system water–NaCl–sucrose is critical for interpreting and understanding the effect of NaCl at a molecular level, even in dry films with moisture content $\leqslant$2 wt %. Samples were thus prepared by adding NaCl to concentrated sucrose aqueous solution and heating to 60 °C to ensure that NaCl was completely dissolved in the sucrose solution.[47] The lack of phase separation (NaCl crystals) in the air-dried mixtures was an indicator of compatibility, suggesting that NaCl affected the physical property of the sucrose matrix through direct interactions between NaCl and sucrose.

There is no particular reason, however, to propose that mobility within the amorphous solid is modulated by a specific complex between NaCl and sucrose. Sucrose can apparently replace water in the hydration sphere of NaCl in aqueous solution[54] and NaCl increases the solubility of sucrose at high concentration of both components,[55] suggesting that non-specific solvation of NaCl ions by sucrose occurs in solution and presumably also in the highly concentrated amorphous solid. Franks and Murase have also reported that NaCl formed a solid solution with sucrose after drying.[56] It is thus plausible to propose that NaCl restricts molecular mobility in the solid matrix by linking sucrose molecules into clusters held together by ion–dipole interactions.

A comparable interaction between citrate carboxylates and sucrose OH, in this case mediated by hydrogen bonds and detected by FTIR, was reported in an amorphous matrix with 0.3 mass fraction citrate/sucrose;[13] it is apparently these interactions that increase T_g by nearly 40 °C. Our studies using Ery B phosphorescence of a sucrose matrix with 0.2 mole ratio sodium citrate/sucrose indicate significantly decreased molecular mobility in both the glass and the undercooled liquid.[42]

3.2. NaCl increased dynamic site heterogeneity in the sucrose matrix

Recent research using a variety of spectroscopic techniques indicates that supercooled liquids and amorphous polymers are dynamically heterogeneous through space at any given time and through time at any give place.[57,58] This physical model is supported by evidence from Ery B phosphorescence where spectral heterogeneity is observed in amorphous sugars and sugar alcohols[29,30,32] and proteins[33,36,37] indicating that the existence of dynamic site heterogeneity may be a characteristic feature of amorphous biomaterials.

In the amorphous sucrose matrix, probe molecules are distributed among dynamically distinct sites with varied emission energies and collisional quenching rates. Pravinata et al. proposed a physical model for this site heterogeneity in which probes in local environments with less

constrained packing have higher overall molecular mobility and thus shorter lifetimes (due to faster collisional quenching) and lower emission energies (due to faster dipolar relaxation).[29]

The variation in the Ery B lifetime with emission wavelength in the glass at 25 °C was slightly greater in sucrose films containing NaCl than in pure sucrose indicating that the distribution of dynamic sites in the sucrose glass was broader in the presence of NaCl. The magnitude of the variation in lifetime with wavelength decreased at high temperature indicating that spectral heterogeneity, and thus dynamic site heterogeneity, decreased in the undercooled liquid.

Two additional spectral parameters also provided evidence for dynamic heterogeneity. Addition of NaCl decreased the stretching exponent β, indicating that NaCl increased the width of the distribution of lifetimes required to describe the intensity decay and thus increased the width of the distribution of sites with different values of k_{TS0}. The values of β were lower in the sucrose–NaCl films than in pure sucrose at temperatures below 85 °C but higher at temperatures above 85 °C, indicating that NaCl increased matrix dynamic heterogeneity in the glass but decreased heterogeneity in the undercooled liquid. The emission bandwidth (Γ) also increased with NaCl content; this effect increased at higher temperatures. The increase in bandwidth in the presence of NaCl reflects an increase in inhomogeneous broadening and thus an increase in the width of the distribution of sites with different interaction energies with the Ery B probe; the variation in interaction energy may reflect variations in dipolar relaxation rate.

All three measures of spectral heterogeneity, lifetime variation with emission wavelength, stretching exponent, and emission bandwidth, thus provide consistent indications that NaCl increased dynamic site heterogeneity in the amorphous sucrose matrix. Such behavior is consistent with the model proposed above in which solvation of NaCl ions by sucrose generates clusters of less mobile molecules. Since the ion–dipole interactions that generate the clusters result from non-specific interactions between sodium and chloride ions and sucrose molecules, the composition of clusters is expected to fall into a random distribution and give rise to greater matrix dynamic heterogeneity.

4. Conclusion

Analysis of the phosphorescence emission energy and lifetime of Ery B in amorphous sucrose and sucrose–NaCl films over the temperature range from 5 °C to 100 °C indicates that addition of NaCl decreases the matrix molecular mobility in both the glass and the undercooled liquid. Three measures of spectral heterogeneity also indicate that addition of NaCl increases the dynamic heterogeneity of the amorphous sucrose. These results are consistent with a physical model in which sodium and chloride ions interact with sucrose OH by ion–dipole interactions, forming clusters of less mobile molecules within the matrix. These results provide valuable insight into the possible role of salts in increasing the stability of biomolecular glasses containing sucrose and other sugars.

5. Experimental

5.1. Sample preparation

Sucrose was purchased from Sigma–Aldrich (St. Louis, MO) with minimum purity of 99.5%. About 50 g of sucrose was dissolved in about 30 g of deionized water containing 0.77 g of activated charcoal to remove luminescent impurities. After stirring overnight, the mixture was vacuum-filtered through ashless filter paper (Whatman No. 40); 0.7 g of activated charcoal was added to the filtrate and the process was repeated. The final concentration of purified sucrose solution was adjusted to 65–67 wt %, confirmed by using a refractometer (NSG Precision Cells, Inc., Farmingdale, NY). Before preparing samples the sucrose solution was filtered through a membrane with 0.2 μm pores to remove any particles.

The free acid of erythrosin B (Ery B, tetra-iodo fluorescein; Sigma Chemical Co., St. Louis, MO) was dissolved in spectrophotometric grade dimethylformamide (DMF; Aldrich Chemical Co., Milwaukee, WI) to prepare a 10 mM stock solution; an aliquot from this solution was added to the concentrated sucrose to obtain a dye/sucrose mole ratio of $1{:}10^4$.

We prepared glassy sucrose films by using a slightly modified version of our previous method.[29] To improve the surface activity for spreading sucrose solutions, quartz slides were washed overnight with Alconox soap, then washed with deionized water, activated for 30 min with concentrated nitric acid, then rinsed with deionized water, and cleaned with 95% EtOH for 2 h and finally with deionized water again. To obtain amorphous sucrose films with Ery B, 15 μL of the sucrose solution containing Ery B at a ratio of $1{:}10^4$ was added on a quartz slide ($30 \times 13.5 \times 0.6$ mm, custom made by NSG Precision Cells, Farmingdale, NY). Another slide was placed on top of the solution and the slides were drawn horizontally past one another to form a film. The solution on the slides was then heated under a heat gun (Vidal Sassoon) for 5 min to a maximum temperature of 86–88 °C (measured using a thermocouple probe). The thickness of amorphous sucrose films prepared by this procedure ranged from 10 to 40 μm. The slides were stored against P_2O_5 and Drie-Rite for at least 7 days and checked for crystals within the film through crossed polarizers in a dissecting microscope

(Nikon Type 102, Japan) before any phosphorescence measurements.

Sucrose–NaCl mixtures were prepared from sucrose solution containing dye. Sodium chloride (99.5% pure; Sigma Chemical Co., St. Louis, MO) was added to the purified sucrose solutions to obtain mixtures with NaCl/sucrose anhydrous mole ratios of 0.04, 0.065, 0.09, 0.20, 0.36, 0.46, 0.56, 0.73, and 0.87. Prior to preparing glassy films, sucrose–NaCl solutions were filtered through a membrane with 0.2 μm pores. The procedure to make a glassy sucrose–NaCl film was the same as the procedure to make a pure sucrose film.

Water content in amorphous sucrose and sucrose–NaCl films was determined gravimetrically (by difference of mass before and after drying for 24 h at 70 °C in an Ephortee (Haake Buchler, Inc.) vacuum oven at 1000 mbar). Sample films were scratched from quartz slides and ground into powders in a glove box containing P_2O_5 and Drie-Rite with a relative humidity less than 5%. Pure sucrose sample contained 0.56 ± 0.13 wt % water, while the NaCl/sucrose samples contained 1.04 ± 0.04, 0.81 ± 0.21, 1.06 ± 0.26, 1.04 ± 0.01, 1.18 ± 0.27, 0.54 ± 0.29, 2.17 ± 0.11, 2.32 ± 0.26, and 2.34 ± 0.25 wt % water for the samples with mole ratios of 0.04, 0.065, 0.09, 0.20, 0.36, 0.46, 0.56, 0.73, and 0.87, respectively.

5.2. Luminescence measurements

Luminescence measurements were made using a Cary Eclipse Fluorescence spectrophotometer (Varian Instruments, Walnut Creek, CA). Prior to any phosphorescence measurements, all samples were flushed for at least 15 min with nitrogen gas, which contained less than 1 ppm oxygen to eliminate oxygen quenching. At each target temperature samples were equilibrated for 1 min/°C increase in temperature. The temperature was controlled using a thermo-electric temperature controller (Varian Instruments, Walnut Creek, CA). To eliminate moisture condensation during the measurements below room temperature, dry air was used to flush the chamber surrounding the cuvette holder. All the measurements were made at least in triplicate.

Delayed fluorescence and phosphorescence emission spectra were collected from 520 to 750 nm (10 nm bandwidth) at 1 nm intervals using excitation of 500 nm (20 nm bandwidth) over a temperature range from 5 to 100 °C with an observation window of 5 ms and an initial delay time of 0.2 ms, which suppresses fluorescence coincident with the lamp pulse. Emission spectra from sucrose or sucrose–NaCl films without probe were subtracted from each spectrum although the background signal was very low.

The energy of the emission maximum (v_p) and the full-width-at-half-maximum (FWHM) of the emission bands was determined by using a log-normal line shape function[59] to fit both delayed fluorescence and phosphorescence.

$$I(v) = I_0 \exp\left\{-\ln(2)\left(\frac{\ln[1 + 2b(v - v_p)/\Delta]}{b}\right)^2\right\} \quad (1)$$

where I_0 is the maximum emission intensity, v_p is the peak frequency (cm^{-1}), Δ is a linewidth parameter and b is an asymmetry parameter. The bandwidth (FWHM; Γ) was calculated according to the following equation:

$$\Gamma = \Delta\left(\frac{\sinh(b)}{b}\right) \quad (2)$$

For delayed luminescence spectra collected from 520 to 750 nm, a sum of log-normal functions for delayed fluorescence ($I_{df}(v)$) and phosphorescence ($I_p(v)$) was used to fit the spectra; each emission band was fit to independent parameters.

Red-edge effect measurements over the temperature range from 5 to 85 °C compared emission energy (Δv_p) with excitation at 530 nm and 560 nm. Phosphorescence emission was collected from 640 to 760 nm using an observation window of 5 ms and 0.1 ms delay. Phosphorescence spectra were converted to intensity versus frequency (cm^{-1}) and analyzed to obtain the peak frequency (v_p) and spectral bandwidth (Γ) using a log-normal function ($I(v)$) (Eq 1).

For lifetime measurements, samples were excited at 530 nm (20 nm bandwidth) and emission transients collected at 680 nm (20 nm bandwidth) over the temperature range from 5 to 100 °C. Phosphorescence intensity decays were collected over a window of 5 ms with an initial delay of 0.1 ms and increments of 0.04 ms. Each decay was the average of 20 cycles. Because intensity decays were non-exponential, a stretched exponential, or Kohlrausch–Williams–Watts' decay function was used to analyze the intensity decay[28,29,60]

$$I(t) = I(0)\exp(-(t/\tau)^{\beta}) + \text{constant} \quad (3)$$

where $I(0)$ is the initial amplitude, τ is the stretched exponential lifetime, and β is an exponent varying from 0 to 1 and characterizing the distribution of lifetimes. The use of a stretched exponential model provides a direct measurement of a continuous distribution of lifetimes, which is appropriate for describing a complex glass possessing a distribution of relaxation times for the dynamic molecular processes. The smaller the β value, the more non-exponential the intensity decays and the broader the distribution of lifetimes. Program NFIT (Galveston, TX) was used to fit the decay; goodness of fit was evaluated by examining the χ^2 and R^2. Plots of modified residuals (the difference between the intensity from the fit decay curve and the measured intensity divided by the square root of the measured intensity) provided an additional indicator of the goodness of fit. R^2 for all fits ranged from 0.99 to 1.00 and

modified residuals plots fluctuated randomly around zero amplitude.

Phosphorescence emission lifetimes of Ery B as a function of emission wavelength were measured with excitation wavelength at 530 nm (20 nm bandwidth); emission wavelength varied from 640 to 720 nm (20 nm bandwidth). Phosphorescence emission lifetimes as a function of excitation wavelength were measured with emission wavelength at 680 nm (20 nm bandwidth); excitation wavelength ranged from 490 to 560 nm (20 nm bandwidth). The experiments were performed at 25 °C.

5.3. Photophysical scheme

Our analysis of the delayed emission is similar to the photophysical scheme for Ery B outlined by Duchowicz et al.[61] and Pravinata et al.[29] The measured emission rate for phosphorescence (k_P) is the sum of all possible deexcitation rates for the triplet state T_1:

$$\tau^{-1} = k_P = k_{RP} + k_{TS1} + k_{TS0} + k_Q[Q] \quad (4)$$

In this equation, k_{RP} is the rate of radiative emission to the ground state S_0, for erythrosin B, k_{RP} is 41 s^{-1} and constant with temperature;[61] k_{TS1} is the rate of thermally activated reverse intersystem crossing from the triplet state T_1 to the singlet state S_1; the value can be estimated from the Arrhenius equation:

$$k_{TS1}(T) = k^0_{TS1} \exp(-\Delta E_{TS}/RT) \quad (5)$$

where k^0_{TS1} is the maximum rate of intersystem crossing from T_1 to S_1 at high temperature, ΔE_{TS} is the energy gap between T_1 and S_1, $R = 8.314$ J K^{-1} mol^{-1}, and T is the temperature in Kelvin. The value of ΔE_{TS} is calculated from the slope of a van't Hoff plot of the natural logarithm of the ratio of intensity of delayed fluorescence (I_{df}) to phosphorescence (I_p):

$$d[\ln(I_{df}/I_P)]/d(1/T) = -\Delta E_{TS}/R \quad (6)$$

where I_{df} and I_p are the maximum intensity values determined from analysis of the emission band using Eq 1. The value of k_{TS1}at 25 °C was estimated as 88 s^{-1} using $k^0_{TS1} = 3.0 \times 10^7$ s^{-1} and $\Delta E_{TS} = 31.56$ kJ/mol.[29]

In the presence of oxygen, the quenching rate $k_Q[Q]$ is the product of rate constant k_Q and the oxygen concentration [O_2]. By flushing nitrogen throughout the measurements we assume that oxygen quenching was negligible. A major non-radiative decay route is by intersystem crossing to the ground state S_0; the decay rate, k_{TS0}, reflects the rate of collisional quenching of the probe due to both internal and external factors.[45] We assume that k_{TS0} primarily reflects external environmental factors since the self-collisional quenching of probe molecules can be neglected within the extremely viscous amorphous solid. In temperature-dependent term k_{TS0} can be calculated from the phosphorescence lifetime by rewriting Eq 4

$$k_{TS0}(T) = \frac{1}{\tau(T)} - k_{RP} - k_{TS1}(T) \quad (7)$$

Acknowledgments

This research was partially supported by funds provided by the CSREES of the US Department of Agriculture, Grant #2002-01585.

References

1. Crowe, J. H.; Carpenter, J. F.; Crowe, L. M. *Annu. Rev. Physiol.* **1998**, *60*, 73–103.
2. Crowe, J. H.; Oliver, A. E.; Tablin, F. *Int. Comp. Biol.* **2002**, *42*, 497–503.
3. Buitink, J.; Leprince, O. *Cryobiology* **2004**, *48*, 215–228.
4. Zallen, R. *The Physics of Amorphous Solids*; John Wiley & Sons: New York, 1983, pp 1–32.
5. Roos, Y. *Phase Transitions in Foods*; Academic Press: San Diego, 1995, pp 193–246.
6. Slade, L.; Levine, H. *Adv. Food Nutr. Res.* **1995**, *38*, 103–269.
7. Fennema, O. R. *Food Chemistry*, 3rd ed.; Marcel Dekker: New York, 1996, pp 17–94.
8. Hofmeister, F. *Arch. Exp. Pathol. Pharmakol.* **1888**, *24*, 247–260.
9. Izutsu, K.; Aoyagi, N. *Intl. J. Pharm.* **2005**, *288*, 101–108.
10. Longinotti, M. P.; Mazzobre, M. F.; Buera, M. P.; Corti, H. R. *Phys. Chem. Chem. Phys.* **2002**, *4*, 533–540.
11. Shalaev, E. Y.; Johnson-Elton, T. D.; Chang, L.; Pikal, M. J. *Pharm. Res.* **2002**, *19*, 195–201.
12. Mazzobre, M. F.; Longinotti, M. P.; Corti, H. R.; Buera, M. P. *Cryobiology* **2001**, *43*, 199–210.
13. Kets, E. P. W.; IJpelaar, P. J.; Hoekstra, F. A.; Vromans, H. *Cryobiology* **2004**, *48*, 46–54.
14. Lu, Q.; Zografi, G. *J. Pharm. Sci.* **1997**, *86*, 1374–1378.
15. Wang, W. *Int. J. Pharm.* **2000**, *203*, 1–60.
16. Wolkers, W. F.; Oldenhof, H.; Alberda, M.; Hoekstra, F. A. *Biochim. Biophys. Acta* **1998**, *1379*, 83–96.
17. Ottenhof, M.; MacNaughtan, W.; Farhat, I. A. *Carbohydr. Res.* **2003**, *338*, 2195–2202.
18. Chan, R. K.; Pathmanthan, K.; Johari, G. P. *J. Phys. Chem.* **1986**, *90*, 6358–6362.
19. Gangasharan; Murthy, S. S. N. *J. Phys. Chem.* **1995**, *99*, 12349–12354.
20. Richert, R. *Europhys. Lett.* **2001**, *54*, 767–773.
21. Kawai, K.; Hagiwara, T.; Takai, R.; Suzuki, T. *Pharm. Res.* **2005**, *22*, 490–497.
22. Shamblin, S. L.; Zografi, G. *Pharm. Res.* **1998**, *15*, 1828–1834.
23. Hancock, B. C.; Shamblin, S. L.; Zografi, G. *Pharm. Res.* **1995**, *12*, 799–806.
24. Roos, Y. H.; Juppila, K.; Zielasko, B. *J. Therm. Anal.* **1996**, *47*, 1437–1450.
25. Van den Dries, I. J.; Besseling, N. A. M.; van Dusschoten, D.; Hemminga, M. A.; van der Linden, E. *J. Phys. Chem. B* **2000**, *104*, 9260–9266.
26. Contreras-Lopez, E.; Champion, D.; Hervet, H.; Blond, G.; Le Meste, M. *J. Agric. Food Chem.* **2000**, *48*, 1009–1015.
27. Buitink, J.; van der Dries, I. J.; Hoekstra, F. A.; Alberda, M.; Hemminga, M. A. *Biophys. J.* **2000**, *79*, 1119–1128.

28. Richert, R. *J. Chem. Phys.* **2000**, *113*, 8404–8429.
29. Pravinata, L. C.; You, Y.; Ludescher, R. D. *Biophys. J.* **2005**, *88*, 3551–3561.
30. Shirke, S.; Ludescher, R. D. *Carbohydr. Res.* **2005**, *340*, 2661–2669.
31. Shirke, S.; Takhistov, P.; Ludescher, R. D. *J. Phys. Chem. B* **2005**, *109*, 16119–16126.
32. Shirke, S.; You, Y.; Ludescher, R. D. *Biophys. Chem.* **2006**, *123*, 122–133.
33. Lukasik, K. V.; Ludescher, R. D. *Food Hydrocolloids* **2006**, *20*, 88–95.
34. Lukasik, K. V.; Ludescher, R. D. *Food Hydrocolloids* **2006**, *20*, 96–105.
35. Simon-Lukasik, K. V.; Ludescher, R. D. *Food Hydrocolloids* **2004**, *18*, 621–630.
36. Nack, T. J.; Ludescher, R. D. *Food Biophys.* **2006**, *1*, 151–162.
37. Sundaresan, K. V.; Ludescher, R. D. *Food Hydrocolloids* **2007**, *22*, 403–413.
38. You, Y.; Ludescher, R. D. *Appl. Spectrosc.* **2006**, *60*, 813–819.
39. Parker, C. A. *Photoluminescence of Solutions*; Elsevier Publishing: Amsterdam, 1968, pp 320–321.
40. Lakowicz, J. R. *Principles of Fluorescence Spectroscopy*; Plenum Press: New York, 1999, pp 237–276.
41. Demchenko, A. P. *Luminescence* **2002**, *17*, 19–42.
42. You, Y. Ph.D. Thesis, Rutgers University, New Brunswick, NJ, 2007.
43. Sun, W. Q.; Leopold, A. C.; Crowe, L. M.; Crowe, J. H. *Biophys. J.* **1996**, *70*, 1769–1776.
44. Urbani, R.; Sussich, F.; Prejac, S.; Cesaro, A. *Thermochim. Acta* **1997**, *304/305*, 359–367.
45. Papp, S.; Vanderkooi, J. M. *Photochem. Photobiol.* **1989**, *49*, 775–784.
46. Fischer, C. J.; Gafni, A.; Steele, D. G.; Schauerte, J. A. *J. Am. Chem. Soc.* **2002**, *124*, 10359–10366.
47. Shalaev, E. Y.; Franks, F. *Thermochim. Acta* **1995**, *255*, 49–61.
48. Shalaev, E. Y.; Franks, F. *J. Phys. Chem.* **1995**, *100*, 1144–1152.
49. Schoorl, N. *Recueil des Travaux Chimiques des Pays-Bas et de la Belgique* **1923**, *42*, 790–799.
50. Vavrinecz, G. *Elelmezesi lpar.* **1958**, *12*, 114–116.
51. Conner, J. M.; Bulgrin, V. C. *J. Inorg. Nucl. Chem.* **1967**, *29*, 1953–1961.
52. Accorsi, C. A.; Bellucci, F.; Bertolasi, V.; Ferretti, V.; Gilli, G. *Carbohydr. Res.* **1989**, *191*, 105–116.
53. Miller, D. P.; de Pablo, J. J.; Corti, H. R. *J. Phys. Chem.* **1999**, *103*, 10243–10249.
54. Mishra, R. G.; Behera, B. *Indian J. Chem., Sect A* **1980**, *19A*, 572–574.
55. Robinson, R. A.; Stokes, R. H.; Marsh, K. N. *J. Chem. Thermodyn.* **1970**, *2*, 745–750.
56. Franks, F.; Murase, N. *Pure Appl. Chem.* **1992**, *64*, 1667–1672.
57. Ediger, M. D. *Annu. Rev. Phys. Chem.* **2000**, *51*, 99–128.
58. Richert, R. *J. Phys. Condens. Mat.* **2002**, *14*, R738–R803.
59. Maroncelli, M.; Fleming, G. R. *J. Chem. Phys.* **1987**, *86*, 6221–6239.
60. Lee, K. C. B.; Siegel, J.; Webb, S. E. D.; Leveque-Fort, S.; Cole, M. J.; Jones, R.; Dowling, K.; Lever, M. J.; French, P. M. W. *Biophys. J.* **2001**, *81*, 1265–1274.
61. Duchowicz, R.; Ferrer, M. L.; Acuna, A. U. *Photochem. Photobiol.* **1998**, *68*, 494–501.